NMR study of magnetic nanoparticles Ni@C

NMR study of magnetic nanoparticles Ni@C

K N Mikhalev[1], A Yu Germov[1], D A Prokopyev[1,2], M A Uimin[1,2], A Ye Yermakov[1,2], A S Konev[1], V S Gaviko[1] and S I Novikov[1]

[1] M.N. Mikheev Institute of Metal Physics, Ural Branch, Russian Academy of Sciences, Yekaterinburg, 620108, Russia
[2] Ural Federal University, Yekaterinburg, 620002, Russia

E-mail: mikhalev@imp.uran.ru

Abstract. The ^{61}Ni, ^{13}C NMR spectra of carbon encapsulated nickel nanoparticles have been obtained. It has been shown that the cores of the particles consist of metallic nickel with face-centered cubic structure, nickel carbide Ni_3C and carbon-nickel solid solution. The carbon shell of nanoparticles is a highly defective structure and close to an amorphous glassy-like carbon.

1. Introduction

Magnetic nanoparticles are of considerable interest both from the fundamental point of view, and with the possibility of their practical application in medicine, spintronics, sensor devices, supercapacitors, catalytic processes, etc. [1-6]. As for medical purposes, it is the most convenient to use nanoparticles in a carbon graphite-like shell, as it is extremely stable under the influence of chemicals and temperature factor [7,8]. On the other hand, the carbon shell is compatible with biological tissues [9].

The properties of these particles depend on many factors: size, phase composition, thickness of the carbon shell, method of synthesis, and so on. In our research the nanocomposites synthesized by the gas-phase method were studied [10].

Experimental methods used to study nanoparticles and nanocomposites usually include both a set of traditional methods (magnetization measurement, x-ray diffraction, neutron diffraction), and local methods (electron microscopy, photoemission spectroscopy, optical methods, EPR, NMR). It should be noted that diffraction methods of structure investigation (x-rays and neutrons) are ineffective for nanoparticles smaller than 10 nm, and the analysis of photoelectron spectra provides only qualitative information [10]. In this case the advantage of local methods is significant [11].

2. Experimental details

Nanoparticles Ni@C were prepared by the gas-phase synthesis. Levitating droplet of liquid nickel was blown around a stream of inert gas (argon) containing hydrocarbons. Nanopowder accumulated on a special filter. Details of the synthesis are available in [12, 13].

The X-ray diffraction patterns of the nanoparticles were measured using a high resolution X-ray diffractometer Empyrean 2 with the Cu K_α radiation. Initial processing, calculation of lattice parameters, and determination of the size of coherent scattering blocks were performed using the HighScore Plus software.

The magnetization has been measured at room temperature using a vibrating sample magnetometer in a magnetic field up to 3 T.

The ^{13}C NMR spectra have been obtained on a Bruker AVANCE 500 pulsed NMR spectrometer in an external magnetic field, H_0 = 11.747 T. The ^{61}Ni NMR signals were detected in H_0 = 0 at a temperature of 4.2 K. A few MHz wide NMR spectrum has been obtained by measuring an integrated intensity of the ^{61}Ni spin echo signals at equidistant ($\Delta\nu$ = 500 kHz) operating frequencies.

3. Results and discussion

According to X-ray diffraction (XRD) data, the average size of nanoparticles is 6 nm. The diffraction peaks correspond only to the face centered cubic (fcc) structure (space group Fm-3m), which refers to the core of the nanoparticles. The unit cell parameter, a = 0.3538(8) nm, is close to a = 0.3531 nm, the lattice constant of a bulk fcc-Ni.

The magnetization reversal curve (figure 1) implies ferromagnetic state of the particles under study. Its sigmoid shape is qualitatively similar to those of nanoparticles with an iron or cobalt core (figure 1). The coercive force is absent ($H_C \approx 0$ Oe). A negligible value of H_C is typical for small particles close to the transition to the superparamagnetic state. However, the magnetization curve cannot be described by the Langevin function (or a superposition of these functions). It is worth noting that the saturation magnetization M_{sat}(Ni@C) = 17.5 emu/g is significantly less than that in pure bulk metallic nickel M_{sat}(Ni) = 55 emu/g [14]. Let us assume that the core with average size 6 nm (see XRD) consists only of the pure nickel and the average thickness of the carbon shell is 1 nm. Then this M_{sat} value corresponds to m_{VCore} = 42.2 at. % (m_{Core} = 77.5 wt. %) of nickel magnetization. Then we should expect the magnetization of the nanoparticles $M_{sat}(Ni@C)_{calc1}$ = 42.6 emu/g which is much higher than the measured value M_{sat}(Ni@C) = 17.5 emu/g. This means that fraction of pure nickel should be much smaller than it follows from the two phase core-shell model. One of the reasonable explanations for such significant reduction of M_{sat}(Ni@C) is probably due to the formation of Ni:C solid solution and/or the formation of nickel-based metastable carbide phases.

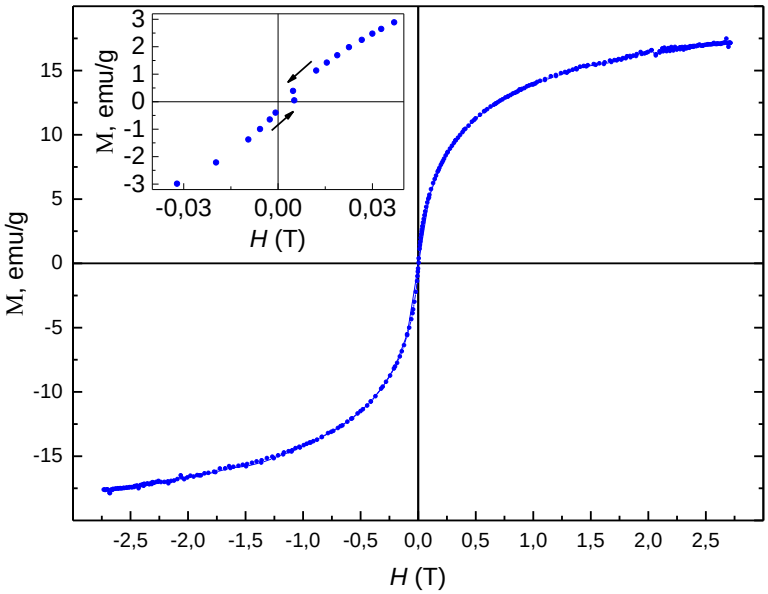

Figure 1. Magnetization reversal curve $M(H)$ of the nickel nanoparticles in carbon shell Ni@C at room temperature. The inset shows an enlarged area near the origin, from which the absence of hysteresis is seen.

The presence of a solid solution and metal-carbon phases with an unknown value of specific magnetization complicates the analysis of the obtained data and leads to ambiguity in the estimates of

the phase composition. In order to establish the presence of additional phases let us turn to the NMR data.

The ^{61}Ni NMR spectrum of Ni@C nanoparticles recorded in a zero external magnetic field consists of several nonhomogeneously broadened lines (figure 2). High amplification factor ($\eta \sim 10^3$) of the obtained ^{61}Ni NMR signals points out to the ferromagnetic state of investigated phases.

The most intensive line in the spectrum (figure 2) with a maximum at 29 MHz corresponds to metallic nickel phase. The absence of quadrupole splitting of the line (^{61}I = 3/2) is evidence of the cubic environment of Ni. Two additional resolved lines in the lower frequency range are attributed to the Ni:C solid solution (maximum of the line near 27 MHz) and nickel carbide Ni_3C (maximum of the line near 24.5 MHz).

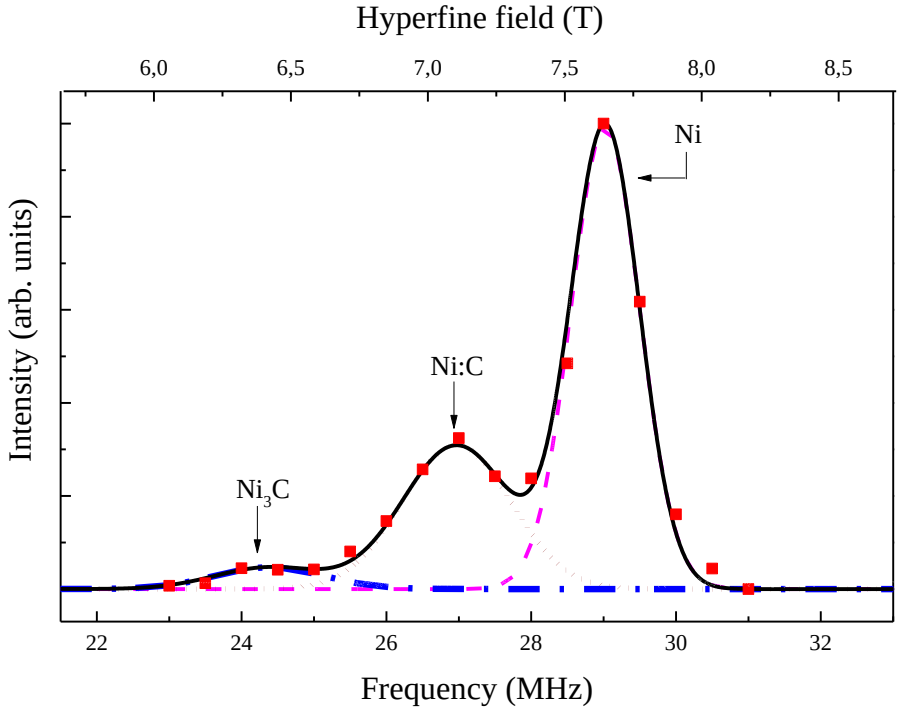

Figure 2. ^{61}Ni NMR spectrum (■) of carbon encapsulated nickel Ni@C nanoparticles obtained at zero external magnetic field at T = 4.2 K. Calculated spectrum (bold line) and the components Ni (dash line), Ni:C (dot line), Ni_3C (dash dot line) are also shown.

Such values of the corresponding induced fields (Table 1) are qualitatively agreed with the values obtained from Mössbauer spectroscopy data [12]. In the case of the formation of a Ni:C solid solution with a different amount of carbon and nickel in the environment and with a different magnetization value and the Curie point, a continuous pedestal would be observed in the spectrum (figure 2) demonstrating the continuous distribution of hyperfine fields. Analysis of the integral intensities of the NMR lines in the spectrum allowed us to determine the concentration of each of the ferromagnetic phases in the core of nanoparticles (table 1).

Table 1. Phase composition obtained according to the ^{61}Ni NMR data for the core of carbon encapsulated nickel nanoparticles Ni@C

Composition	Central transition frequency (MHz)	Hyperfine field (T)	Fraction of ferromagnetic phases at 4.2 K (at. %)
Ni (metallic)	29 ± 0.2	7.6 ± 0.2	56 ± 3
Ni_xC (solid solution)	26.9 ± 0.2	7.1 ± 0.2	37 ± 3
Ni_3C (carbide)	24.3 ± 0.2	6.4 ± 0.2	7 ± 3

The ^{13}C NMR spectrum shows the nonhomogeneous broadened line (figure 3).

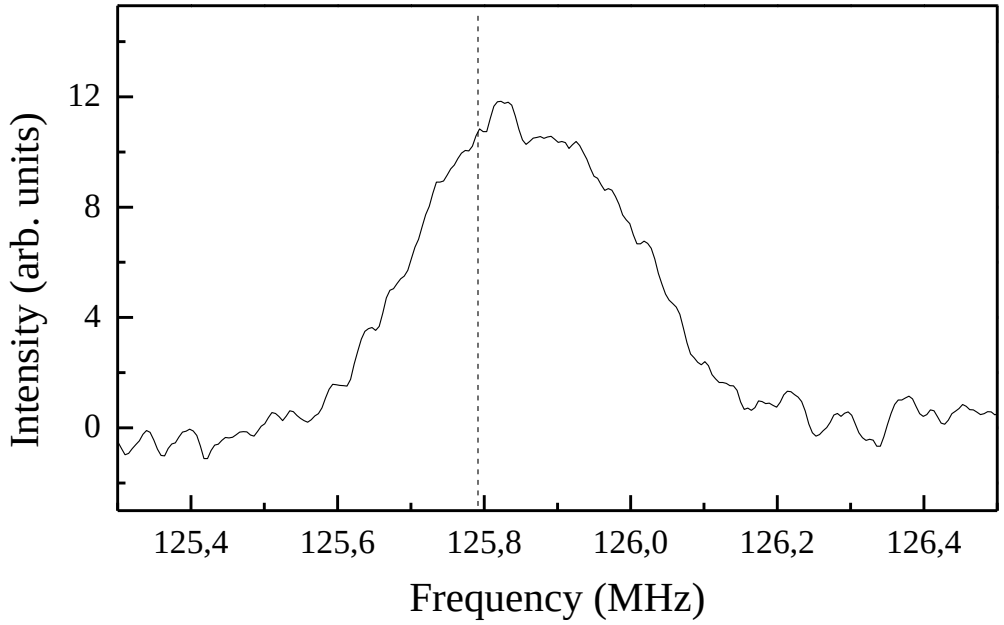

Figure 3. ^{13}C NMR spectrum of Ni@C nanoparticles obtained at magnetic field H_0 = 11.747 T at T = 295 K. Dashed line shows the value of diamagnetic point (zero shift) of ^{13}C.

It drastically differs from the narrow lines of graphene or graphite [16]. A similar spectrum was observed in carbon encapsulated cobalt nanoparticles Co@C [13] prepared following the same procedure. Thus, we may conclude that the carbon shell of the investigated nanoparticles consists of amorphous glass-like carbon.

4. Summary

The ^{61}Ni, ^{13}C NMR spectra of nanoparticles Ni@C have been firstly obtained and analyzed. On the basis of the joint analysis of the ^{61}Ni NMR data, XRD, magnetization and electron microscopy, the phase composition and average size of nanoparticles have been determined. It has been shown that the NMR method has found phases which may not be detected by the XRD method in small nanoparticles. According to ^{13}C NMR data, the carbon shell of the studied nanoparticles is most likely to consist of amorphous glassy-like carbon.

Acknowledgments
The study was performed within the state assignments of the Mikheev Institute of Metal Physics of the Ural Branch of the Russian Academy of Sciences: state program «Function» No AAAA-A19-119012990095-0; state program «Magnit» No AAAA-A18-118020290129-5 and state program «Alloys». The research also was supported by the project of the complex program of Ural Branch of Russian Academy of Sciences № 18-10-2-37.

References

[1] Sharoyan E G, Mirrahkanyan A A, Gyulasaryan H T, Kocheryan A N and Makuryan A S 2017 *J. of Contemporary Phys.* **52** 147

[2] Erokhin A V, Lokteva E S, Yermakov A Ye, Bukhvalov D W, Maslakov K I, Golubina E V and Uimin M A 2014 *Carbon* **74** 291

[3] Xiong W, Zhou Y S, Hou W J, Guillemet T, Silvain J F, Gao Y, Lahaye M, Lebraud E, Xu S, Wang X W, Cullen D A, More K L, Jiang L and Lu Y F 2015 *RSC Adv.* **5** 99037

[4] Huba Z J and Carpenter E E 2014 *Dalton Trans.* **43** 12236

[5] Jiao M, Li K, Guan W, Wang Y, Wu Z, Page A and Morokuma K 2015 *Scientific Reports* **5** 12091

[6] Bayer B C, Bosworth D. A., Michaelis F B, Blume R, Habler G, Abart R, Weatherup R S, Kidambi P R, Baumberg J J, Knop-Gericke A, Schloegl R, Baehtz C, Barber Z H, Meyer J C and Hofmann S 2016 *J. Phys. Chem. C* **120** 22571

[7] Xiaoling G, Xiao C, Dangsheng S and Changhai L 2018 *Acta Chim. Sinica* **76** 22

[8] Guo Q, Guo Z, Shi J, Sang L, Gao B, Chen Q, Liu Z and Wang X 2018 *MRS Communications* **8** 88

[9] Solovyev A A, Oskomov K V, Grenadyorov A S and Maloney P D 2018 *Thin Solid Films* **650** 37

[10] Galakhov V R, Shkvarin A S, Semenova A S, Uimin M A, Mysik A A, Shchogoleva N N, Yermakov A Ye and Kurmaev E Z 2010 *J. Phys. Chem.* **114** 22413

[11] Mikhalev K N, Germov A Yu, Yermakov A E, Uimin M A, Buzlukov A L and Samatov O M 2017 *Physics of the Solid State* **59** 514

[12] Tsurin V A, Yermakov A Ye, Uimin M A, Mysik A A, Shegoleva N N, Gaviko V S and Maikov V V 2014 *Physics of the Solid State* **56** 287

[13] Mikhalev K N, Germov A Yu, Uimin M A, Yermakov A E, Konev A S, Novikov S I, Gaviko V S and Ponosov Yu S 2018 *Mater. Res. Express* **5** 055033

[14] Graham C D 1982 *Journal of Applied Physics* **53** 2032

[15] Fujieda S, Kuboniwa T, Shinoda K, Suzuki S and Echigoya J 2016 *AIP Advances* **6** 056116.

[16] de Souza F A L 2016 *J. Phys. Chem.* C **120** 27707